

14B.4 THE DEPENDENCE OF THE MICROWAVE EMISSIVITY OF THE OCEAN ON HURRICANE FORCE WIND SPEED

Chris Ruf^{1*}, Amanda Mims¹ and Chris Hennon²

¹University of Michigan, Ann Arbor, MI, ²University of North Carolina Asheville, Asheville, NC

1. ABSTRACT

The WindSat fully polarimetric microwave radiometer has been in orbit since 2003. WindSat's ability to satisfactorily retrieve wind vector at wind speeds below 20 m/s and through clear air and light precipitation has been well documented in the refereed literature (Mondaldo, 2006; Brown *et al.*, 2006). Its sensitivity to wind direction in much higher (hurricane force) winds has also recently been demonstrated (Yueh, 2006). Results are presented here of a study which examines WindSat's sensitivity to wind speed in hurricanes. The study involves an intercomparison between WindSat overpass measurements, made during 2005 of Hurricanes Dennis, Rita and Katrina, and surface wind fields for those overpasses, generated using NOAA's H*Wind system. Collocation between the wind field and emissivity retrieved from the brightness temperature and the "ground truth" provided by H*Wind shows a well-behaved and monotonic dependence of emissivity on wind speed even in hurricane force winds.

Section 2 presents the motivation for our study. Section 3 describes the datasets from WindSat and the H*Wind analysis in detail. The atmospheric clearing method used for extraction of surface emissivity from observed top of atmosphere radiance is given in Section 4. Finally, Section 5 explores the results of the data comparison.

2. MOTIVATION

The microwave emissivity of the ocean surface is affected by the presence of foam. Foam acts like a near-perfect blackbody and therefore has an emissivity close to unity. This forces its brightness temperature to be significantly warmer than the surrounding foam-free ocean. The fraction of the surface covered by foam is monotonically related to near surface wind speed. As wind speed increases, the sea surface is roughened and the foam coverage increases as well. This raises the emissivity of the surface and; hence the observed brightness temperature. This process has been well documented for wind speeds below 20 m/s and serves as the basis for numerous successful wind speed retrieval algorithms [ref].

The purpose of this study is to document the behavior of ocean surface emissivity at winds above 20 m/s in extreme weather conditions. The chosen situation for these conditions is a tropical cyclone, which is accompanied by wind speeds up to 70 m/s as well as heavy precipitation. A potential fault in the proposed system may occur in such high winds; the wind speeds will eventually become strong enough to cover the entire surface in question with foam. At this point, it becomes

impossible to detect any higher wind speeds. It is necessary for the value of radiometric high wind retrieval that this saturation point not occur at or before 30 m/s, a Category 1 hurricane. This exploration seeks to show that the foam fraction does not saturate before this point.

3. DATASETS

Our study involved two main sources of data: the WindSat brightness temperatures hosted by Colorado State University (CSU) and the H*Wind analysis (Powell *et al.* 1998) as utilized by the National Oceanic and Atmospheric Administration (NOAA). The ocean surface wind speed is calculated from the temperature set and compared to H*Wind, which serves as our observed wind speed.

3.1 WINDSAT OBSERVATIONS

The WindSat satellite orbits the Earth in LEO, making full revolutions every 90 minutes. Raw WindSat observations consist of fully polarimetric top-of-atmosphere radiances at 10.7, 18.7 and 37.0 GHz and dual linear polarization radiances at 6.8 and 23.8 GHz (Gaiser *et al.*, 2004). The higher frequency vertically polarized channels are relatively insensitive to surface wind effects and so are used to estimate the absorbing and emitting atmospheric water vapor and liquid constituents between the satellite and the surface. Once the atmosphere has been characterized, its effects on the radiance at all frequencies and polarizations can be removed from those observations and the underlying ocean surface emissivity can be derived. That emissivity is then matched up against corresponding H*Wind surface wind speeds. This study focuses on the sensitivity of vertically and horizontally polarized surface emissivity to wind speed in tropical cyclones. The sensitivity of the 3rd and 4th Stokes parameters to wind direction has been addressed previously (Yueh, 2006).

Three WindSat overpasses of tropical cyclones during the active 2005 hurricane season were chosen for our study. In each case, the satellite overpass occurred more than 100 km from any shoreline in order to reduce the effects of land brightness contamination. The first overpass is of cyclone Dennis on 9 July 2005. The second occurred on 28 August 2005 of cyclone Katrina, just hours before it made landfall. The third storm overpass is of Rita on 21 September 2005. An example of the brightness temperature measured by WindSat during its Katrina overpass is shown in Figure 1. The image is by the 37 GHz vertically polarized channel.

* C. Ruf, Dept. of AOSS, Univ. of Michigan, 2455 Hayward St., Ann Arbor, MI 48109-2143, cruf@umich.edu

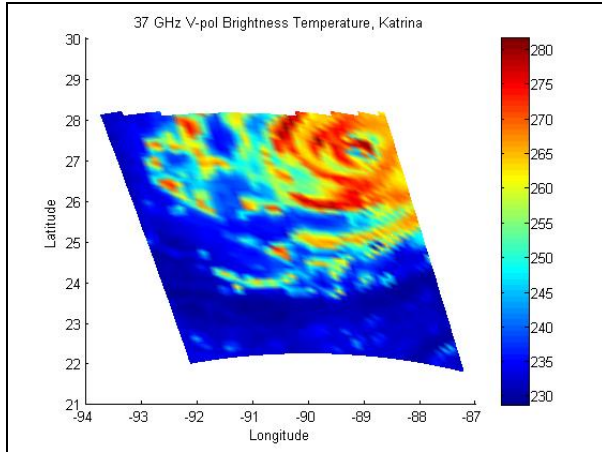


Figure 1. WindSat 37 GHz V-pol brightness temperature (K) during overpass of tropical cyclone Katrina on 28 August 2005.

3.2 H*WIND SURFACE WIND FIELDS

H*Wind is a tool that provides an objective analysis of the tropical cyclone surface wind field by assimilating all available surface observations, as well as aircraft and remotely sensed data, into a common framework that also allows for human quality control. The H*Wind algorithms, graphical user interface, and databases were developed over a number of years at the NOAA Hurricane Research Division (HRD) and have been used for post-storm analysis and to experimentally support operational cyclone analysis. All data included in an analysis are transformed into a storm relative coordinate system. In this research, the storm centers are linearly interpolated from the surrounding 'best track' fixes from the National Hurricane Center (NHC).

3.3 WIND SPEED VALIDATION

Caution has to be used when applying an H*Wind analysis for wind speed validation purposes. Due to a lack of data at any one time, H*Wind is not a snapshot of the wind field; rather, it is an assimilation of observations that have been collected during a three to six hour period. Further, much of the storm circulation remains unobserved even by including data over such a time window. Since the wind field structure of a typical tropical cyclone is highly variable in both space and time, a significant error range in the analysis field is introduced. Typical wind speed errors in an H*Wind analysis are estimated to be 10%-20% (Houston et al. 1999), although that will vary depending on the quantity and quality of data that are available as well as the degree of quality control employed by the analyst. In particular, H*Wind maximum wind values are usually lower than the actual intensity of the cyclone due to under sampling of the cyclone circulation and the smoothing performed by the objective analysis.

We were careful to choose three cases where the cyclone was well sampled around the WindSat pass time. We selected Dennis (2246 UTC 9 July 2005),

Observation Platform	Dennis (July 9, 2246 UTC)		Katrina (Aug. 28, 2349 UTC)		Rita (Sept. 21, 2257 UTC)	
	Number Obs.	Time Range	Number Obs.	Time Range	Number Obs.	Time Range
AFRES	642	18:16 – 01:30	0		692	18:00 – 23:55
SFMR	357	18:52-22:30	2021	19:00 – 01:20	310	18:00 – 21:00
Moored Buoy	325	18:19-01:30	0		385	18:09 – 03:00
QuikSCAT	0		818	23:49 – 23:51	554	23:27 – 23:30
GOES cloud drift winds	270	19:02 – 22:02	0		149	19:02 – 22:02
GPS Dropsonde	6	18:15 – 23:10	8	20:41 – 02:35	34	18:03 – 01:19
Ship	27	18:18 – 1:00	0		22	18:17 – 01:01

Table 1. Observation platforms used by H*Wind to produce the wind validation fields.

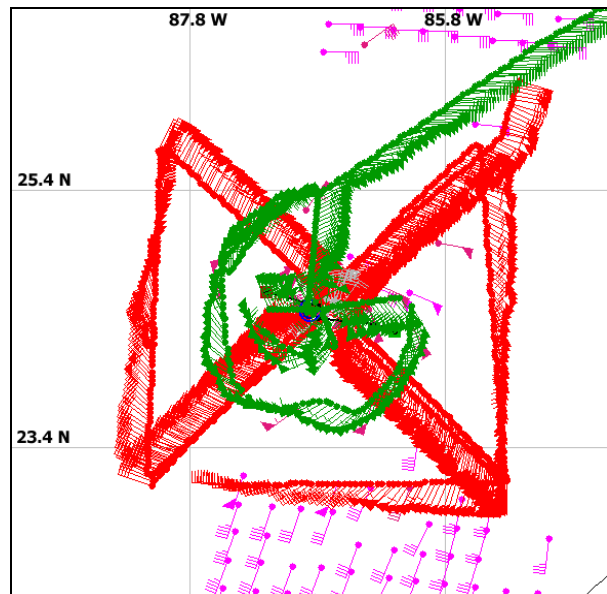


Figure 2. Observations that were assimilated into the H*Wind system for Hurricane Rita at 2257 UTC 21 September 2005. Data were collected from 1800 UTC through 0000 UTC on 22 September. See Table 1 for a listing of specific data sources utilized.

Katrina (2147 UTC 28 August 2005), and Rita (2257 UTC 21 September 2005) as suitable candidates for a wind speed comparison. In Table 1, details about each of the analyses are given, including the type and amount of data that contributed to the wind field. The amount of data available for each pass was sufficient for a reasonable wind speed analysis. All three storms were sampled by Stepped Frequency Microwave Radiometer (SFMR, Uhlhorn and Black 2003) wind retrievals and Global Positioning Satellite (GPS) dropsondes (which provide vertical profiles of several variables, including wind speed and direction from flight level to just above the surface). Air Force Reconnaissance flight level winds (AFRES) are

automatically reduced to a 10 m near surface wind through standard techniques. The spatial coverage of the tropical cyclones was excellent, as shown in Hurricane Rita in Figure 2 – the other two storms had similar coverage. In H*Wind, all data are transformed to a uniform 1-minute average and 10 m height.

4. ATMOSPHERIC CLEARING AND SURFACE EMISSIVITY ESTIMATOR

The method used to extract estimates of ocean surface emissivity from observations of top of atmosphere brightness temperature was first developed in Brown *et al.* (2006) and is summarized here. The observed brightness temperature can be expressed as

$$T_B(f, p, \theta) = \varepsilon(f, p, \theta) T_{surf} e^{-\tau(f) \sec \theta} + T_{up}(f, \theta) + \Gamma (T_{down}(f, \theta) + T_{cosmic} e^{-\tau(f) \sec \theta}) e^{-\tau(f) \sec \theta} \quad (1)$$

where θ is the incidence angle, f is the frequency and p is the polarization. T_{surf} denotes sea surface temperature and T_{cosmic} the cosmic background brightness temperature, both given in K. T_{up} and T_{down} are also in K, and represent the atmospheric upwelling and downwelling brightness temperatures, respectively. Their specific forms are as described in Brown *et al.* (2006). ε is the ocean surface emissivity, Γ is the surface reflectivity and τ is the atmospheric optical depth.

The first step is to estimate optical depth by an iterative least squares inversion of Eq. (1). The inversion process must simultaneously estimate surface emission and reflection. A subset of the WindSat channels (higher in frequency and vertically polarized only) are used to maximize sensitivity to the atmosphere and minimize sensitivity to the surface. These model used for surface emissivity is based on Wilheit (1979), which assumes a combination a rough ocean surface over which is fractional foam coverage. The surface emissivity model is given by

$$\varepsilon(W) = \varepsilon_0 + a_0 (1 - \exp[-a_1 W - a_2 W^2]) \quad (2)$$

where W is wind speed in m/s and ε_0 is calm (specular) sea surface emissivity. The coefficients in the model are listed in Table 2 for each WindSat channel.

Atmospheric optical depth is parameterized as a function of the column integrated water vapor and cloud and rain liquid water. The model relating them is given by

$$\tau(f) = c_{0,f} + c_{1,f} V + c_{2,f} L \quad (3)$$

where V is integrated water vapor burden, L is integrated liquid water content, and the coefficients are listed in Table 3.

Inversion of Equation (1) returns two primary quantities: water vapor (cm) and liquid water (mm), and retrieves wind speed as a secondary object. Figure 4 displays the retrieved liquid water for the Katrina overpass. In the figure, the eye is centered in the upper

	a_0	a_1 (m/s) ⁻¹	a_2 (m/s) ⁻²
6.8 H-pol	0.246	1.03E-03	6.80E-04
6.8 V-pol	0.163	3.52E-04	4.75E-04
10.7 H-pol	0.269	2.35E-04	1.30E-03
10.7 V-pol	0.176	1.09E-04	1.01E-03
18.7 H-pol	0.462	3.71E-03	8.64E-04
18.7 V-pol	0.202	1.11E-04	1.03E-03
23.8 H-pol	0.440	2.46E-05	1.35E-03
23.8 V-pol	0.224	1.95E-04	1.00E-03
37 H-pol	0.495	4.16E-04	9.90E-04
37 V-pol	0.216	1.68E-04	8.96E-04

Table 2. Coefficients for Equation (4.2), an emissivity model dependent solely on wind speed.

	c_0	c_1 (cm) ⁻¹	c_2 (mm) ⁻¹
6.8 GHz	1.024E-02	0	1.020E-02
10.7 GHz	1.222E-02	7.230E-04	2.385E-02
18.7 GHz	1.819E-02	1.484E-02	6.972E-02
23.8 GHz	2.340E-02	5.210E-02	0.1103
37 GHz	6.190E-02	1.137E-02	0.2491

Table 3. Coefficients for optical depth parameterization. Revised from version found in Brown *et al.* (2006).

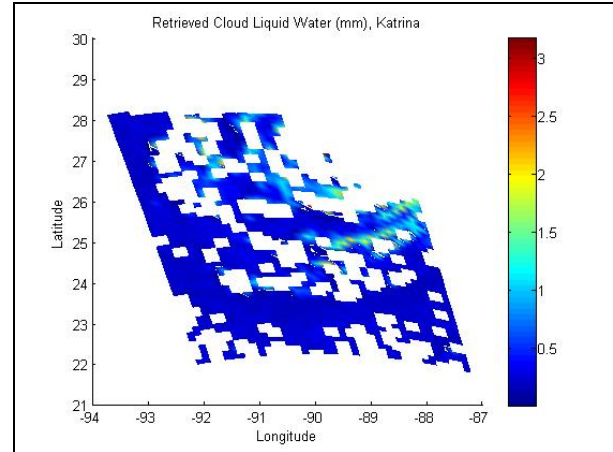


Figure 4. Image of cloud liquid water (mm) retrieved from WindSat brightness temperature for Katrina overpass. Data gaps (white regions) in image indicate improper retrievals. Eye of cyclone located in upper right portion of image.

right portion of the image. The distinctive spiral rainbands of the storm are visible in the image. Data gaps (white regions) result when the inversion either does not converge, converges with an unreasonably high residual X2 fit between the observations and the estimate of the observations given the solution, or converges to non-physical values for the retrieved geophysical parameters. These situations tend to happen in areas where the rain is extremely intense, suggesting that the forward model may be inadequate.

The current forward model does not include the effects of scattering from suspended ice particles above the rain, or from the rain itself, which should become much more significant in high rain conditions. This is an area for future development of the atmospheric clearing algorithm.

Once estimates are available of the integrated water vapor and liquid water content, the optical depth at any frequency or polarization can be estimated using equation. In particular, the surface emissivity can be derived for the 6.8 and 10.7 GHz WindSat channels.

The final emissivity results are compared to the appropriate H*Wind surface wind field.

5. RESULTS – RESPONSE OF SURFACE EMISSIVITY TO HIGH WINDS

The collocation between the WindSat retrieved sea surface emissivity and the H*Wind wind field for each of the three overpass cases is shown in Figure 5 for the 6.8 GHz horizontal polarization channel. The data is color coded to show which cyclone it comes from, and it is clear that the surface emissivity relation to wind speed follows the same trend for each storm. Below 30 m/s, the comparison is consistent with previously published results for the relationship between wind speed and surface emissivity. The emissivity then continues to increase as the wind speed rises well past 30 m/s. Any possible saturation in this behavior does not begin until at least 50 m/s.

These results indicate that the foam fraction of the surface does not saturate until well above 30 m/s. Emissivity values are still sensitive to the wind speed at hurricane force wind speeds. Therefore, it is reasonable to assume microwave radiometry is a valid method for tracking intense storm formations into the tropical cyclone range. The Saffir-Simpson Hurricane Scale denotes 33 m/s to 42 m/s as a Category 1 storm, and 42 m/s to 50 m/s as a Category 2 storm. As shown in Figure 5, the emissivity relation is sensitive to wind speeds reaching into this range. WindSat appears to be capable of tracking these storms and their wind speed distributions. At the time of satellite overpass, storms Katrina and Rita were in the Category 3 range and Dennis was in the Category 1 range. This leads to a scarcity of extremely high wind data. As such, further examination of stronger storms will determine WindSat's proficiency in higher category cyclones.

In order to increase confidence in our results, steps are currently being taken to match the footprints of each WindSat channel data before re-implementing the model process. This will ensure that all retrieved surface emissivity signals are purely the result of wind speed and foam fraction, and are not artifacts of spatial misalignment. Nevertheless, our preliminary results indicate that there is a noticeable trend between wind speed and emissivity, and it can be used to great advantage in microwave radiometry from space.

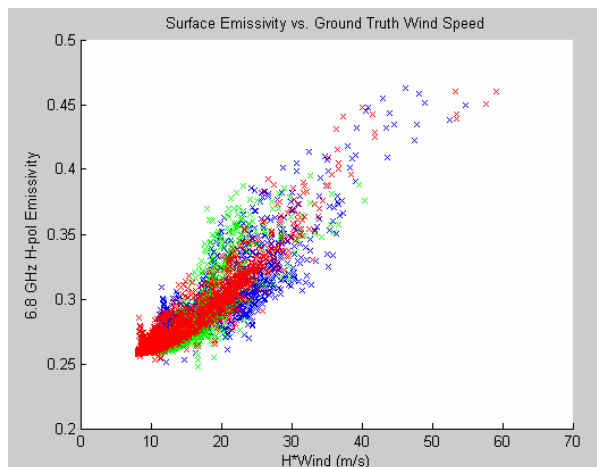


Figure 5. Sea surface emissivity vs. wind speed. Emissivity derived from 6.8 GHz H-pol WindSat channel, wind speed from collocated H*Wind analysis. Red data points from cyclone Katrina. Green data points from cyclone Dennis. Blue data points from cyclone Rita.

6. SUMMARY

Spaceborne microwave radiometers can be extremely valuable both for scientific study and for tracking atmospheric conditions. For example, radiometric retrieval of general ocean surface wind speeds is reliable and well understood. However, its capability for unusual and extreme conditions has not been examined in depth as of yet. Our study addresses this issue, using tropical cyclones to provide the necessary dynamic conditions. Such situations include high winds up to 70 m/s as well as heavy precipitation.

The data used in our study is taken from WindSat's observations of three cyclones during the 2005 season: Dennis, Katrina and Rita. H*Wind surface wind fields are composed for these specific cases and used as the observed wind distribution. Brightness temperatures from WindSat are subjected to our emissivity retrieval model, based mainly on the inversion of a forward model with the radiative transfer equation.

Our results show the relationship between ocean wind speed and surface emissivity. The monotonic trend between emissivity, which is dependent on the surface foam fraction, and wind speed, which is the foam driver, is viably extended beyond 30 m/s into the tropical cyclone range. The foam fraction of a windy ocean does not saturate before the cyclone wind speed range, allowing radiometers such as WindSat to correctly retrieve wind values even into intense storms.

7. REFERENCES

- Brown, S.T., Ruf, C.S., Lyzenga, D.R., 2006: An Emissivity-Based Wind Vector Retrieval Algorithm for the WindSat Polarimetric Radiometer. *IEEE Trans. Geosci. Remote Sens.*, **44**, 611-621.

- Gaiser, P.W., K.M. St. Germain, E.M. Twarog, G.A. Poe, W. Purdy, D. Richardson, W. Grossman, W.L. Jones, D. Spencer, G. Golba, J. Cleveland, L. Choy, R.M. Bevilacqua and P.S. Change, 2004: The WindSat polarimetric spaceborne microwave radiometer: Sensor description and early orbit performance, *IEEE Trans. Geosci. Remote Sens.*, **42**(11), 2347-2361.
- Houston, S.H., W.A. Shaffer, M.D. Powell, and J. Chen, 1999: Comparisons of HRD and SLOSH surface wind fields in hurricanes: Implications for storm surge modeling. *Weather and Forecasting*, **14**, 671-686.
- Monaldo, F.M., 2006: Evaluation of WindSat wind vector performance with respect to QuikScat estimates, *IEEE Trans. Geosci. Remote Sens.*, **44**(3), 638-644.
- Powell, M.D., S.H. Houston, L.R. Amat, and N. Morisseau-Leroy, 1998: The HRD real-time hurricane wind analysis system. *Journal of Wind Engineering and Industrial Aerodynamics*. **77&78**, 53-64.
- Uhlhorn, E.W., and P.G. Black, 2003: Verification of remotely sensed sea surface winds in hurricanes. *Journal of Atmospheric and Oceanic Technology*, **20**, 99-116.
- Wilheit, T.T., 1979: A Model for the Microwave Emissivity of the Ocean's Surface as a Function of Wind Speed. *IEEE Transactions on Geoscience and Remote Sensing*, **GE-17**, 244-249.
- Yueh, S., July 2006: Polarimetric Microwave Remote Sensing of Hurricane Ocean Winds, *Proc. IGARSS 2006*, Denver, CO.